Loss of *PTEN* sensitizes head and neck squamous cell carcinoma to 5-AZA-2'-deoxycytidine

Gabriell Bonifacio Borgato, DDS, PhD,[a,b] Gabriel Alvares Borges, DDS, PhD,[b,c] Ana Paula Souza, DDS, PhD,[a] Cristiane Helena Squarize, DDS, PhD,[b,d] and Rogerio Moraes Castilho, DDS, PhD[b,d]

Objective. Head and neck squamous cell carcinoma (HNSCC) is an aggressive cancer associated with poor survival. Phosphatase and tensin homolog (*PTEN*) is a tumor suppressor gene involved in the maintenance of stem cells. DNA methylation is a known epigenetic modification involved in tumor progression. In this study, we investigated the effect of the DNA demethylation agent 5-AZA-2′-deoxycytidine (5-AZA) over HNSCC and its population of cancer stem cells (CSCs) presenting dysfunctional *PTEN*.

Study Design. The effects of 5-AZA on HNSCC were evaluated by using WSU-HN13 cells. CSC was assessed by sphere-forming assays, along with the endogenous levels of aldehyde dehydrogenase. The clonogenic potential of tumors was evaluated, along with the protein expression of mTOR signaling and the identification of nuclear factor-κB (NF-κB) and epithelial–mesenchymal transition (EMT)–associated genes, using real-time polymerase chain reaction (PCR).

Results. We observed that loss of *PTEN* enhances tumor biologic behavior, including colony- and tumor sphere–forming abilities. We also found that 5-AZA has an inhibitory effect over the CSCs and molecular markers associated with the NF-κB and EMT pathways.

Conclusions. Our findings suggest that the stratification of treatment of HNSCC based on PTEN status may identify a subset of patients who can benefit from the coadministration of 5-AZA. (Oral Surg Oral Med Oral Pathol Oral Radiol 2020;130:181–190)

Head and neck squamous cell carcinoma (HNSCC) is the most common malignancy of the head and neck anatomic area. Although early diagnosis of HNSCC is often associated with a good prognosis, tumors are typically identified at advanced stages, with local and distant metastases, and present an unfavorable prognosis. Surgical procedures are often extensive, resulting in a high degree of morbidity.[1] Radiotherapy and chemotherapy are often employed in the treatment of advanced-stage cancers[2]; however, the efficacy of therapy is dampened by the frequent development of tumor chemoresistance. Emerging evidence suggests that cancer stem cells (CSCs) play an important role in the development of a tumor-resistant phenotype. This is particularly true because of the slow-cycling nature of CSCs, along with activation of resistance-associated pathways, such as the nuclear factor-κB (NF-κB) signaling pathway.[3-6]

The phosphatase and tensin homolog (*PTEN*) gene is a tumor suppressor and a master regulator of the phosphoinositide 3-kinase pathway and the mammalian target of rapamycin (mTOR) signaling pathway.[7] Reduced levels of the PTEN protein or mutations on the *PTEN* gene are commonly observed events in solid tumors, such as HNSCCs, glioblastomas, and cancers of the breast, endometrium, and prostate.[8-12] Compromised expression levels of the PTEN protein are observed in nearly 31% of HNSCCs and up to 50% of all advanced cases.[13-17] Part of *PTEN* involvement in tumor progression may be linked to its regulatory function over epithelial stem cells.[18] As in normal epithelial stem cells, *PTEN* is also involved in the accumulation of CSCs in a variety of tumors, including breast cancer and HNSCCs.[19,20] CSCs are known for their ability to resist chemotherapy, thereby conferring a resistant phenotype to tumors.

Recent reports have described the involvement of epigenetic modifications, such as DNA methylation, histone modifications, chromatin remodeling, and noncoding RNA, during carcinogenesis and tumor progression.[21] These epigenetic modifications contribute to the acquisition of cellular plasticity and the self-renewing properties of cancer cells.[22] DNA methylation is one of the most studied epigenetic modifications in mammals. In normal cells, DNA methylation represents one of the mechanisms responsible for the maintenance of adequate gene expression.[23,24] In tumor cells, hyper-

Statement of Clinical Relevance

Cancer stem cells (CSCs) are involved in tumor progression, invasion, and chemoresistance. We found that the demethylation agent 5-AZA is particularly effective in depleting CSC from *PTEN*-deficient tumors.

[a]Department of Oral Biology, School of Dentistry, State University of Campinas, Piracicaba, São Paulo, Brazil.
[b]Laboratory of Epithelial Biology, Department of Periodontics and Oral Medicine, School of Dentistry, University of Michigan, Ann Arbor, MI, USA.
[c]Laboratory of Oral Histopathology, Health Sciences Faculty, University of Brasilia, Brasilia, Brazil.
[d]University of Michigan Comprehensive Cancer Center, Ann Arbor, MI, USA.

Received for publication Sep 15, 2019; returned for revision Mar 23, 2020; accepted for publication May 3, 2020.

2212-4403/$-see front matter
https://doi.org/10.1016/j.oooo.2020.05.001

methylation is a common event involved in the loss of function of tumor suppressor genes. Mechanistically, DNA methylation is a reversible enzymatic process, which can be modulated by epigenetic drugs.[25] Epigenetic drugs, such as histone deacetylase inhibitors and DNA demethylation agents,[26,27] have been used in an attempt to reactivate silenced tumor suppressor genes. 5-AZA-2'-deoxycytidine (5-AZA) is a nucleoside analogue that is incorporated into DNA as an adduct and binds an irreversible manner with DNA methyltransferase enzymes. Consequently, 5-AZA-DNA binding causes enzyme degradation, leading to a cascade of demethylation effect on DNA.[26,27]

In this study, we observed that HNSCC cells presenting loss of *PTEN* are endowed with a higher potential for colony formation and generation of tumor spheres. Epigenetic interference of tumor DNA methylation with the use of 5-AZA was able to reduce the colony-forming potential of HNSCC cancer cells, independent of the activation status of the *PTEN* gene. Administration of 5-AZA was also effective in downregulating holoclone formation while inducing the accumulation of meroclones and paraclones in *PTEN* knockdown (KD) cells. We further observed that the administration of 5-AZA differentially impacts genes associated with the NF-κB and the epithelial−mesenchymal transition (EMT) pathways from *PTEN* wildtype (WT) and KD tumor cells. Finally, we observed that *PTEN* KD CSCs presented sensitivity to 5-AZA compared with WT cells. Altogether, our findings demonstrate that HNSCC tumors presenting loss of *PTEN* are particularly sensitive to 5-AZA.

MATERIALS AND METHODS

Cell culture

The squamous cell carcinoma cell line WSU-HN13 (RRID: CVCL_5519) was cultured in DMEM (Dulbecco's modified Eagle medium; Hyclone Laboratories Inc., Logan, UT) and supplemented with 10% bovine serum (Thermo Scientific, Rockford, IL), and penicillin (100 U/mL)−streptomycin (100 μg/mL) (Invitrogen, Carlsbad, CA) and incubated at 37°C and 5% carbon dioxide. All experiments were conducted using 10^4 cells/mL.

5-AZA treatment

Cells were seeded in 100-mm Petri dishes for colony and tumor sphere assays, 6-well plates for gene expression assays, and 24-well plates for inhibition of *PTEN* with interference RNA and aldehyde dehydrogenase (ALDH) activity. After 24 hours, the cells were exposed to 1-μM 5-AZA (Invitrogen, Carlsbad, CA) for 48 hours without medium exchange.

siRNA knockdown, short hairpin RNA, plasmids, and lentivirus

The knockdown of *PTEN* was performed by using small interfering RNA (siRNA) as previously described.[18,19] Briefly, cells were seeded in 24-well plates and transfected with 12.5-nM double-stranded RNA oligonucleotides directed against human *PTEN* (NM_000314; forward: 5'- CCA AUG GCU AAG UGA AGA UGA CAA U [dT] [dT]-3' and reverse: 5'-AUU GUC AUC UUC ACU UAG CCA UUG G [dT] [dT] -3') (Invitrogen, Carlsbad, CA). Optimal concentrations and time points were determined by dilution curves of siRNA for each target and immunoblot analyses. The sequences of the negative control siRNA (Invitrogen, Carlsbad, CA) oligonucleotides were as follows: 5'-UUC UCC GAA CGU GUC ACG UdTdT-3' and 5'-ACG UGA CAC GUU CGG AGA AdTdT-3'. Lentiviral vectors (pGIPZ) expressing *PTEN* short hairpin RNA or empty vector pGIPZ expressing control short hairpin RNA (Dharmacon, Lafayette, CO) were used as previously described.[28] Briefly, HEK 293 T cells were transfected with psPAX2 and pMD2 G plasmids (Addgene; Trono Lab, Watertown, MA), supernatant medium containing lentivirus was collected (72 hours), and WSU-HN13 cells were transduced in the presence of 4 mg/mL polybrene (Millipore Sigma, Burlington, MA). Positive cells for the transduced vector were selected by using 1 mg/mL of puromycin (Millipore Sigma, Burlington, MA).

RNA extraction and reverse transcription

Cell RNA was extracted by using the Quick-RNA MicroPrep Kit (Zymo, Irvine, CA), which has an extra step of genomic DNA digestion. After extraction, RNA was quantified by fluorometry with the Qubit apparatus (Thermo Scientific, Rockford, IL). For complementary DNA (cDNA) synthesis, the High Capacity cDNA Reverse Transcription Kit (Thermo Scientific, Rockford, IL) was used with 1 μg of RNA.

Quantitative real-time polymerase chain reaction

For the quantification of expression of genes related to the NF-κB pathway (*TNF-α, IL6, IL1 β, IL10, IRAK3*, and *MAVS*), tumor stem cell status (*SNAI1* and *c-MYC*), *NDRG2*, and *PTEN*, Green Mastermix (Thermo Scientific, Rockford, IL) with the thermocycler of the 7900 HT Real-time PCR System (Applied Biosystems, Foster City, CA), 250 nM of each primer and 2 μL of cDNA were used for a final volume of 10 μL per reaction. Polymerase chain reaction (PCR) conditions were: 95°C for 10 minutes, 40 cycles at 95°C for 15 seconds, 60°C for 20 seconds, and 72°C for 30 seconds. After obtaining the amplification results, relative gene expression levels were calculated by using the $2^{-\Delta\Delta CT}$ method.[29] Initially, the amplification values of the

target genes of each group were normalized by the reference gene (*GAPDH*), and then the normalized values of each experimental group were compared with the values of the control group. Primer sequences were collected from the Primer Bank database[30] and are described as follows:

Gene	Forward 5' ≥ 3'	Reverse 5' ≥ 3'
GAPDH	ACCCACTCCTCC ACCTTTGAC	CCACCACCCTGT TGCTGTAG
TNF-α	GAGGCCAAGCC CTGGTATG	CGGGCCGATTGA TCTCAGC
IL-6	ACTCACCTCTTC AGAACGAATTG	CCATCTTTGGAAGG TTCAGGTTG
IL-1 B	TTCGACACATGG GATAACGAGG	TTTTTGCTGTGAGT CCCGGAG
IL-10	TCAAGGCGCAT GTGAACTCC	GATGTCAAACTCACT CATGGCT
IRAK3	CAGCCAGTCTG AGGTTATGTTT	TTGGGAACCAACTTT CTTCACA
MAVS	TTCTAATGCGCT CACCAATCC	CCATGCTAGTAGGCA CTTTGGA
SNAI1	GCGTGTGCTCG GACCTTCT	ATCCTGAGCAGCCGG ACTCT
c-MYC	GGCTCCTGGCA AAAGGTCA	CTGCGTAGTTGTGCT GATGT
NDRG2	CTGGAACAGCTA CAACAACC	TCAACAGGAGACCTC CATGG
PTEN	TGGATTCGACTT AGACTTGACCT	GCGGTGTCATAATGTC TCTCAG

Western blotting

Tumor cells were lysed with cell lysis buffer containing protease inhibitors and briefly sonicated. Total protein was run in sodium dodecyl sulfate−polyacrylamide gel electrophoresis and transferred to an Immobilon membrane (Millipore, Billerica, MA). Membranes were blocked in 5% nonfat dry milk containing 0.1 M Tris (pH 7.5), 0.9% sodium chloride and 0.05% Tween-20 for 1 hour at room temperature. Membranes were incubated with anti-PTEN (9559 S, 1:1000, 54 kDa; Cell Signaling, Danvers, MA), phospho-s6 ser 235/236 (4857 S, 1:1000, 34 kDa; Cell Signaling, Danvers, MA), NDRG2 (5667 S, 1:1000, 45 kDa; Cell Signaling, Danvers, MA), DNMT1 (20701, 1:500, 183 kDa; Santa Cruz Biotechnology, Santa Cruz, CA), phospho-AKT ser 473 (9271 S, 1:1000, 60 kDa; Cell Signaling, Danvers, MA), and GAPDH (CB1001, 1:20000, 37 kDa; Millipore, Billerica, MA) primary antibodies at 4°C overnight. Membranes were then incubated with appropriate secondary antibodies conjugated to horseradish peroxidase (Santa Cruz Biotechnology, Santa Cruz, CA). Western blotting was developed by using the ECL Western Blotting Substrate (Pierce Biotechnology, Rockford, IL).

Flow cytometry

CSCs from WSU-HN13 transfected with siRNA were identified by the coexpression of ALDH and CD44 using flow cytometry. Briefly, the Aldefluor kit (StemCell Technologies, Durham, NC) was used to identify the high enzymatic activity of ALDH. The specific inhibitor of ALDH diethylaminobenzaldehyde was used as a negative control, according to the manufacturer's recommendations. CD44 antibody conjugated with APC (Clone G44-26, 1:100; BD Biosciences, San Jose, CA) was used in combination with the Aldefluor kit. Samples were analyzed by using the Accuri C6 Plus flow cytometer (BD Biosciences, San Jose, CA). ALDH activity was analyzed on the fluorescein isothiocyanate channel and CD44 on the allophycocyanin channel. CSCs were identified through expression of the high enzymatic activity of ALDH and the high protein levels of CD44.

Colony formation

For colony formation, 400 cells were seeded per well (n = 12) and maintained for 7 days. After this period, the cells were washed, fixed with methanol/acetic acid, and stained with crystal violet. The plates were scanned and the colonies counted with Image J software. A minimum of 50 cells was needed to be considered a colony formed by a clone. Densitometry was performed with the aid of the software and the ratio values normalized by GAPDH.

Tumor sphere formation

For tumor spheres formation, 2500 cells per well (n = 12) were seeded into 6-well plates of low adhesion (Corning, Corning, NY) and were maintained for 5 days. Next, tumor spheres were counted with the aid of an inverted microscope according to the holoclone, meroclone, and paraclone phenotypes.

Statistical Analysis

Statistical analyses were performed by using GraphPad Prism software, version 8. The statistical tests used were the 1-way analysis of variance and the Student *t* test. The results are represented by the mean ± SEM. Asterisks denote a significant statistical difference (* $P \leq .05$; ** $P \leq .01$; *** $P \leq .001$; **** $P \leq .0001$; and NS $P > .05$).

RESULTS

Loss of function of the tumor suppressor gene *PTEN* enhances the aggressiveness of HNSCC.

PTEN function is regulated by several mechanisms, including phosphorylation, ubiquitination, oxidation, and acetylation.[31] In this study, we used WSU-HN13 cells transduced with shPTEN to explore the impact of the loss of *PTEN* in the biology of HNSCC. We found

that loss of *PTEN* (shPTEN) resulted in the increased foci formation of tumor cells compared with empty vector-transduced cells (pGIPZ) (Figures 1A and 1B; ***$P < .0001$). Using sphere-forming assay, we also observed that the absence of *PTEN* resulted in the accumulation of holoclones and paraclones in WSU-HN13 tumor cells (Figure 1C and 1D; ** $P < .01$; ***$P < .001$). However, more differentiated tumor spheres, called *paraclones*, were not influenced by *PTEN* depletion (see Figure 1D; NS $P > .05$). Interestingly, we observed that *PTEN* depletion from HNSCC resulted in the accumulation of NDRG2, a coadjutant protein responsible for promoting *PTEN* function by preventing its phosphorylation (Figure 1E). This finding likely reveals a feedback mechanism that aims at upregulating *PTEN* levels, here artificially driven by short hairpin. Downregulation of *PTEN* also resulted in activation of the PI3K/AKT/mTOR promitogenic and oncogenic pathways, as demonstrated by the accumulation of the phosphorylated S6 (ser235/236) protein, a marker for mTOR activation, and the accumulation of phosphorylated AKT (ser473) (see Figure 1E). At the gene levels, we observed that *PTEN* disruption resulted in the accumulation of proinflammatory genes associated with the NF-κB signaling pathways, including *TNF-α, IL-1β, IL10, IRAK3*, and *MAVS*, along with EMT markers, such as *c-MYC* and *SNAI1*.[32,33] Together with the reduced expression of *PTEN*, we observed upregulation of the *NDRG2* gene, similar to our protein data[34-36] (Figure 1F). The presence of CSCs is a factor known to be associated with aggressive tumor behavior and potential resistance to chemotherapy.

Administration of 5-AZA has a long-term inhibitory effect over HNSCC colony formation and selectively disrupts holoclones.

DNA methylation is an important event in the carcinogenesis of solid tumors, such as HNSCCs, because it reduces the expression of tumor suppressor genes through the hypermethylation of the promoter region.[37] Changes in the DNA methylation landscape leads to the proliferation of tumor cells, along with enhanced tissue invasion, evasion of apoptosis, and metastasis.[38] Interference with the global methylation status of tumor cells can be achieved by inducing hypomethylation of DNA with the use of 5-AZA.[23,24] In our study, we explored the effects of a single administration of 5-AZA on HNSCC behavior (Figure 2A). We found that 5-AZA is efficient in reducing the colony-forming ability of both HNSCC expressing normal levels of *PTEN* and tumor cells depleted of *PTEN* (Figures 2B and 2C; ** $P < .01$). We have previously shown that HNSCC tumor spheres differ in their behaviors, depending on size and shape.[39] Although holoclones present a greater degree of aggressiveness and a higher number of ALDH and CD44 positive tumor cells, meroclones and paraclones are considered to have less "stemness" potential and present reduced aggressive behavior.[39] A sphere-forming assay using HNSCC cells transduced with empty vector (pGIPZ) or with shPTEN revealed that holoclones are particularly sensitive to 5-AZA (Figures 2D and 2E; *** $P < .001$; **** $P < .0001$). Meroclones and paraclones derived from control tumor cells did not respond to 5-AZA therapy (see Figure 2D; NS $P > .05$). Unexpectedly, we observed a significant increase in the number of meroclones and paraclones derived from *PTEN*-depleted HNSCC upon administration of 5-AZA (see Figure 2E; * $P < .05$; **** $P < .0001$). Although the molecular mechanism associated with *PTEN*-driven accumulation of meroclones and paraclones remains unknown, *PTEN*-deficient tumors present a distinct control over the formation of tumor spheres.

Loss of *PTEN* sensitizes genes associated with NF-κB and EMT signaling pathways to 5-AZA therapy

In our study, we decided to explore the impact of 5-AZA administration on HNSCC presenting normal expression levels of the *PTEN* gene and its counterpart tumor cells presenting *PTEN* loss of function. From a gene expression perspective, we observed that loss of *PTEN* sensitizes the NF-κB–associated genes *TNF-α, IL1β, IL10, IRAK3,* and *MAVS* to 5-AZA, but we did not observe downregulation of *IL6* (Figure 3A). In fact, similar findings have been observed in chronic inflammatory diseases and cancers, in which downregulation of *PTEN* is linked to the upregulation of *IL6*.[40,41] Interestingly, only the genes *IL1β* and *IL10,* which were found in control tumor cells, were downregulated with 5-AZA. We have previously shown that high expression levels of NF-κB are directly associated with tumor resistance to therapy on HNSCC cells.[4] Similar to the NF-κB pathway–associated genes, *c-MYC, SNAI1,* and *TNF-α* were also downregulated in *PTEN*-deficient cells upon administration of 5-AZA (see Figure 3A; Figures 3B and 3C). From a PI3K/AKT/mTOR perspective, loss of *PTEN* (PTEN-KD) resulted in the accumulation of NDRG2, pS6, pAKT, and DNMT1 (Figure 3D; vehicle group). The effects of 5-AZA over PI3K/AKT/mTOR signaling was also evident. Administration of 5-AZA resulted in significant accumulation of NDRG2, pS6, and pAKT in PTEN-WT cells. Interestingly, the administration of 5-AZA had a different effect over PTEN-KD cells, in which the NDRG2 and DNMT1 protein levels were found to be diminished, whereas the pS6 and pAKT protein levels remained the same (see Figure 3D; PTEN-KD group). The global DNA demethylation induced by the administration of 5-AZA also caused a reduction in the number of CSCs in HNSCC, presenting loss of *PTEN* as judged by the

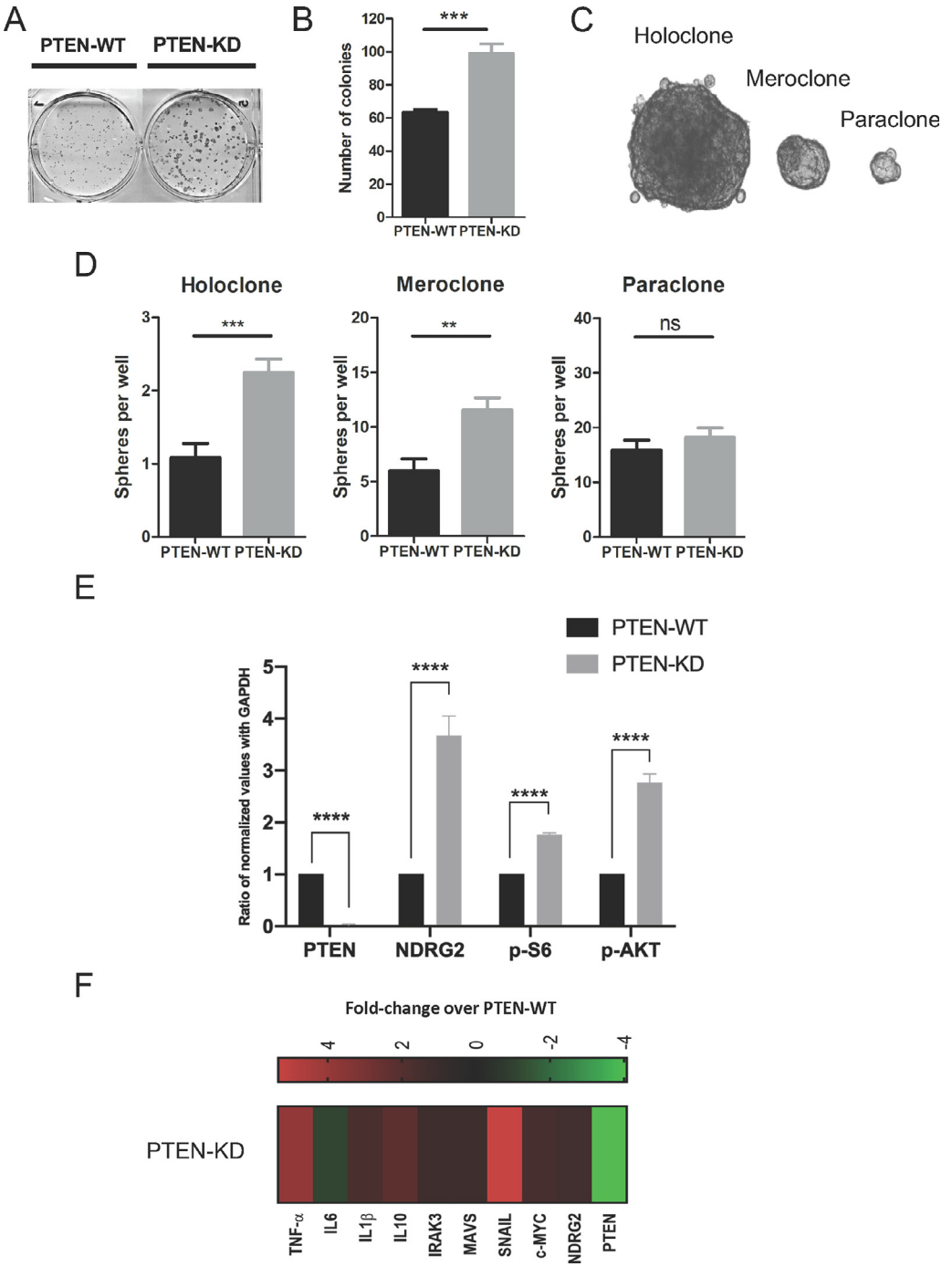

Fig. 1. *PTEN* loss of function induces an aggressive phenotype in head and neck squamous cell carcinoma (HNSCC). **(A, B)** Colony-forming capacity after phosphatase and tensin homolog (*PTEN*) loss of function in HNSCC cells. Note the enhanced capacity in short hairpin PTEN (shPTEN) HNSCC cells (PTEN-KD) (*** $P < .001$). **(C, D)** Representative tumor sphere phenotypes in light microscopy (10 x magnification) and graphical representation of each type. PTEN loss of function enriched for holoclone (*** $P < .001$) and paraclone (** $P < .01$) types. **(E)** Protein quantification of Western blot showing the accumulation of NDRG2 after *PTEN* silencing. Also, note the activation of PI3K/AKT/mTOR with the accumulation of phosphorylated S6 and phosphorylated AKT. **(F)** Heatmap representing gene expression fold change after *PTEN* silencing, normalized by GAPDH expression. Note the upregulation of tumor necrosis factor-α (TNF-α) and SNAI1.

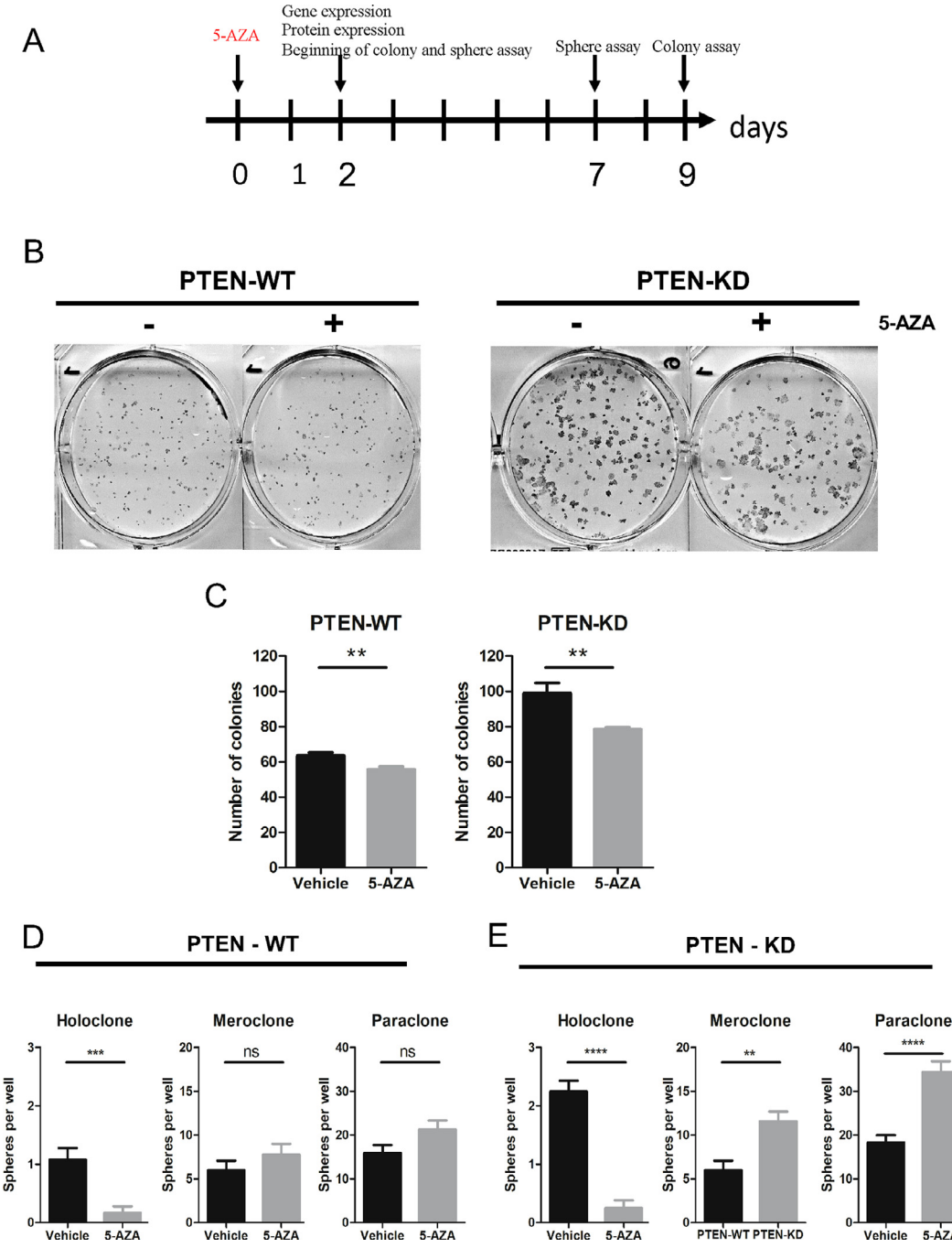

Fig. 2. 5-AZA-2'-deoxycytidine (5-AZA) inhibits colony formation and disrupts holoclone tumor sphere. **(A)** Schedule of 5-AZA administration and experiment time points. **(B, C)** Inhibition of colony formation after 5-AZA administration in both normal phosphatase and tensin homolog (*PTEN*) expression (** $P < .01$) and *PTEN* silencing (** $P < .01$). **(D, E)** Tumor sphere quantification shows disruption of holoclone types after 5-AZA administration (*** $P < .001$; **** $P < .0001$). Meanwhile, with *PTEN* silencing, an enrichment for meroclone (* $P < .05$) and paraclone (**** $P < .0001$) was observed.

levels of ALDH ^{bright} CD44^{+} positive cells (Figures 3E and 3F).

In summary, the long-term effects of 5-AZA in HNSCC are centered on the reduction of colony-forming cells along with a reduced number of holoclones, independent of the *PTEN* status. However, loss of *PTEN* does impact the genetic profiling of genes associated with NF-κB signaling and the accumulation of ALDH^{bright} CD44^{+} CSCs. Altogether, our findings suggest that *PTEN* status in HNSCC changes tumor behavior and response to DNA demethylation therapies.

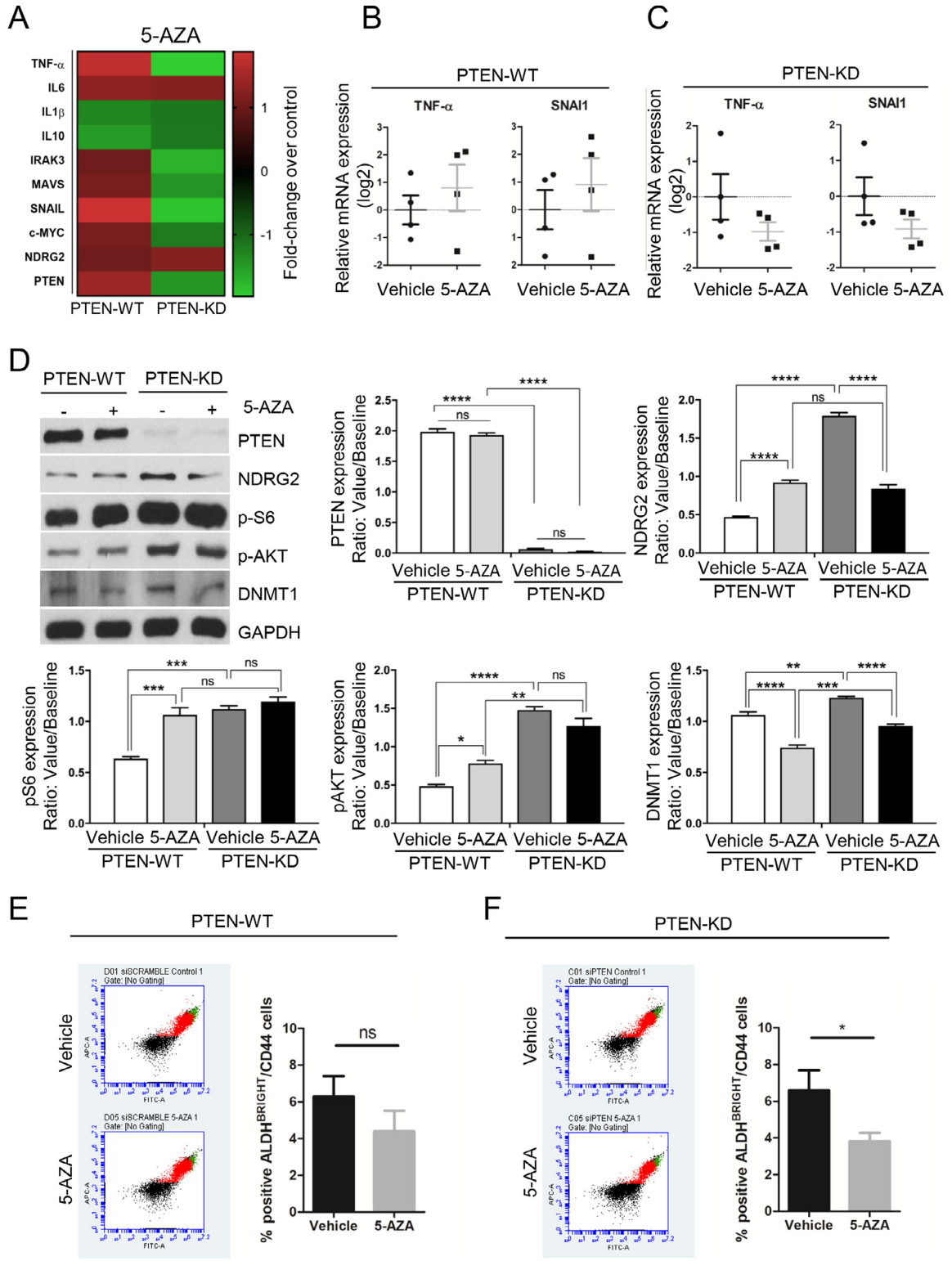

Fig. 3. Phosphatase and tensin homolog (*PTEN*) silencing favors 5-AZA-2'-deoxycytidine (5-AZA) therapy for cancer stem cell (CSC) inhibition. **(A)** Heatmap representing fold change in gene expression of pGIPZ and shPTEN WSU-HN13 cells, with GAPDH as the reference gene after 5-AZA treatment. **(B, C)** Dot plot highlighting the gene expression variation of nuclear factor-κB (NF-κB) and EMT markers tumor necrosis factor-α (TNF-α) and SNAI1 after administration of 5-AZA, in PTEN-WT (wild type) and PTEN-KD (knockdown) tumors. Note that 5-AZA targets NF-κB and EMT markers when PTEN is silenced. **(D)** Protein levels of PTEN, NDRG2, *P*-S6, *P*-AKT, and DNMT1 upon administration of 5-AZA to PTEN-WT and PTEN-KD tumor

DISCUSSION

Many molecular mechanisms are associated with the cellular transformation and progression of solid tumors. Among several mechanisms, loss of function of tumor suppressor genes plays an important role in tumor formation. Mutations are the major driving cause of loss of function of tumor suppressor genes; however, emerging data suggest that epigenetic modifications, including DNA hypermethylation, can also dampen the protective function of tumor suppressor genes in HNSCC. *PTEN* is a tumor suppressor gene that plays an important role in controlling the oncogenic PI3 K/mTOR signaling pathway. Most recently, *PTEN* has been shown to control epithelial stem cell homeostasis[18] and CSCs from cancers of epithelial origin, including breast, thyroid, and hair follicle tumors.[42] The loss of the protective function of *PTEN* in the oral cavity has also been shown to contribute to the formation of oral cancer in an animal model of HNSCC.[15] In our study, we found that HNSCC tumors presenting loss of *PTEN* function do present a growth advantage over HNSCC tumors containing wild-type *PTEN*. The depletion of *PTEN* also facilitates the accumulation of tumor spheres, along with the overexpression of oncogenic PI3K/ATK/mTOR signaling. A similar accumulation of CSCs upon *PTEN* depletion has been shown in breast cancer.[20,43]

One of the interesting findings of our study is the identification of the family members of the NF-κB signaling pathway that are upregulated upon *PTEN* depletion. Activation of NF-κB signaling is known to lead to tumor resistance to chemotherapy and to enrich the population of CSCs in different solid tumors, including mucoepidermoid carcinomas,[44,45] and squamous cell carcinomas.[4,46] It is interesting to note the direct effect of *PTEN* depletion and the accumulation of CSCs, along with the upregulation of the NF-κB pathway, suggesting a synergism between the PI3K and the NF-κB signaling. Nonetheless, the molecular circuitry involved in *PTEN* and NF-κB signaling remain poorly understood. Some reports show that activation of NF-κB signaling leads to the downregulation of *PTEN* in non−small cell lung cancer and thyroid cancer cells.[47,48] However, other studies in prostate cancer have demonstrated an indirect effect of *PTEN* signaling over the NF-κB pathway mediated by the inhibition of TNF.[49] As previously mentioned, activation of NF-κB signaling is associated with the development of tumor resistance to chemotherapy. This is the case in non−small cell lung cancer, in which loss of *PTEN* function leads to activation of NF-κB signaling, along with the acquisition of a phenotype resistant to cisplatin.[50] The findings of these studies, together, support our findings in the PTEN−NF-κB signaling axis in solid cancers. Furthermore, the development of a resistance phenotype driven by the loss of *PTEN* and upregulation of NF-κB also implies the possible accumulation of CSCs. The role of CSCs in tumor resistance to therapy is an emerging field of research.[51-53]

Along with the *PTEN*-driven upregulation of NF-κB signaling, we decided to explore the impact of a global demethylation agent on HNSCC tumor biology. Demethylation agents are often used in cancer therapy to reduce or ablate the hypermethylation status of tumor suppressor genes. In our study, we created a *PTEN*-depleted cell line that resembles *PTEN* mutation in head and neck tumors. Although we did not expect any influence of 5-AZA over *PTEN* levels, it became clear that the process of DNA demethylation was very effective in downregulating NF-κB signaling from *PTEN*-depleted tumors. Along with the downregulation of NF-κB signaling, the administration of 5-AZA also led to a reduction in the population of CSCs exclusively from *PTEN*-depleted cells. The ability of demethylation agents to deplete CSCs has been demonstrated in other solid tumors[54-58]; however, the observation that loss of *PTEN* results in sensitization of CSCs to 5-AZA is a novel concept that has not been elucidated by previous research. It is important to note that our study used only one HNSCC cell line, and although we have found similar trends in stem cell accumulation upon *PTEN* downregulation/depletion, the results presented here should be carefully interpreted.

CONCLUSIONS

The findings of this study suggest that stratification of treatment for HNSCC based on *PTEN* status may identify a subset of patients who can benefit from the coadministration of 5-AZA.

FUNDING

This work was conducted during the period as a visiting scholar at the University of Michigan, sponsored by the Capes Foundation within the Ministry of Education, Brazil (grant No. BEX / 88881.132588/2016-01; grant No. BEX / 88881.187926/2018-01). This study was funded by the University of Michigan School of Dentistry faculty grant. The funders had no role in

cells. **(E, F)** CSC population represented in the scatter plot of fluorescence-activated cell sorting (FACS) analysis, with fluorescein isothiocyanate (FITC) channel representing $ALDH^{BRIGHT}$ intensity and APC channel representing CD44 positive intensity. Only the cells positive for both staining were considered cancer stem cells (CSCs). Note that 5-AZA inhibits the population of CSCs only when *PTEN* is silenced (* $P < .05$).

study design, data collection, and analysis, decision to publish, or preparation of the article.

REFERENCES

1. Molinolo AA, Amornphimoltham P, Squarize CH, Castilho RM, Patel V, Gutkind JS. Dysregulated molecular networks in head and neck carcinogenesis. *Oral Oncol*. 2009;45:324-334.
2. Vigneswaran N, Williams MD. Epidemiologic trends in head and neck cancer and aids in diagnosis. *Oral Maxillofac Surg Clin North Am*. 2014;26:123-141.
3. Castilho RM, Squarize CH, Almeida LO. Epigenetic modifications and head and neck cancer: implications for tumor progression and resistance to therapy. *Int J Mol Sci*. 2017:18. pii: E1506.
4. Almeida LO, Abrahao AC, Rosselli-Murai LK, et al. NF-κB mediates cisplatin resistance through histone modifications in head and neck squamous cell carcinoma (HNSCC). *FEBS Open Bio*. 2014;4:96-104.
5. Monisha J, Roy NK, Bordoloi D, et al. Nuclear factor kappa B: a potential target to persecute head and neck cancer. *Curr Drug Targets*. 2017;18:232-253.
6. Rayet B, Gelinas C. Aberrant *rel/nfkb* genes and activity in human cancer. *Oncogene*. 1999;18:6938-6947.
7. Wang X, Jiang X. Post-translational regulation of *PTEN*. *Oncogene*. 2008;27:5454-5463.
8. Lui VW, Hedberg ML, Li H, et al. Frequent mutation of the PI3 K pathway in head and neck cancer defines predictive biomarkers. *Cancer Discov*. 2013;3:761-769.
9. Poetsch M, Lorenz G, Kleist B. Detection of new *PTEN/MMAC1* mutations in head and neck squamous cell carcinomas with loss of chromosome 10. *Cancer Genet Cytogenet*. 2002;132:20-24.
10. Li J, Yen C, Liaw D, et al. *PTEN*, a putative protein tyrosine phosphatase gene mutated in human brain, breast, and prostate cancer. *Science*. 1997;275:1943-1947.
11. Tashiro H, Blazes MS, Wu R, et al. Mutations in PTEN are frequent in endometrial carcinoma but rare in other common gynecological malignancies. *Cancer Res*. 1997;57:3935-3940.
12. Djordjevic B, Hennessy BT, Li J, et al. Clinical assessment of *PTEN* loss in endometrial carcinoma: immunohistochemistry outperforms gene sequencing. *Mod Pathol*. 2012;25:699-708.
13. Giudice FS, Squarize CH. The determinants of head and neck cancer: unmasking the PI3 K pathway mutations. *J Carcinog Mutagen*. 2013;Suppl 5. pii: 003.
14. Squarize CH, Castilho RM, Santos Pinto D Jr. Immunohistochemical evidence of *PTEN* in oral squamous cell carcinoma and its correlation with the histological malignancy grading system. *J Oral Pathol Med*. 2002;31:379-384.
15. Squarize CH, Castilho RM, Abrahao AC, Molinolo A, Lingen MW, Gutkind JS. *PTEN* deficiency contributes to the development and progression of head and neck cancer. *Neoplasia*. 2013;15:461-471.
16. Lee JI, Soria JC, Hassan KA, et al. Loss of *PTEN* expression as a prognostic marker for tongue cancer. *Arch Otolaryngol Head Neck Surg*. 2001;127:1441-1445.
17. Shao X, Tandon R, Samara G, et al. Mutational analysis of the *PTEN* gene in head and neck squamous cell carcinoma. *Int J Cancer*. 1998;77:684-688.
18. Zagni C, Almeida LO, Balan T, et al. *PTEN* mediates activation of core clock protein BMAL1 and accumulation of epidermal stem cells. *Stem Cell Rep*. 2017;9:304-314.
19. Matsumoto CS, Almeida LO, Guimaraes DM, et al. PI3 K-*PTEN* dysregulation leads to mTOR-driven upregulation of the core clock gene *BMAL1* in normal and malignant epithelial cells. *Oncotarget*. 2016;7:42393-42407.
20. Sun L, Burnett J, Gasparyan M, et al. Novel cancer stem cell targets during epithelial to mesenchymal transition in *PTEN*-deficient trastuzumab-resistant breast cancer. *Oncotarget*. 2016;7:51408-51422.
21. Baylin SB, Jones PA. Epigenetic determinants of cancer. *Cold Spring Harb Perspect Biol*. 2016;8. pii: a019505.
22. Reya T, Morrison SJ, Clarke MF, Weissman IL. Stem cells, cancer, and cancer stem cells. *Nature*. 2001;414:105-111.
23. Li E, Zhang Y. DNA methylation in mammals. *Cold Spring Harb Perspect Biol*. 2014;6. pii: a019133.
24. Schubeler D. Function and information content of DNA methylation. *Nature*. 2015;517:321-326.
25. Kulis M, Esteller M. DNA methylation and cancer. *Adv Genet*. 2010;70:27-56.
26. Ghoshal K, Datta J, Majumder S, et al. 5-AZA-deoxycytidine induces selective degradation of DNA methyltransferase 1 by a proteasomal pathway that requires the KEN box, bromo-adjacent homology domain, and nuclear localization signal. *Mol Cell Biol*. 2005;25:4727-4741.
27. Christman JK. 5-Azacytidine and 5-AZA-2'-deoxycytidine as inhibitors of DNA methylation: mechanistic studies and their implications for cancer therapy. *Oncogene*. 2002;21:5483-5495.
28. Nascimento-Filho CHV, Webber LP, Borgato GB, Goloni-Bertollo EM, Squarize CH, Castilho RM. Hypoxic niches are endowed with a protumorigenic mechanism that supersedes the protective function of *PTEN*. *Faseb J*. 2019;33:13435-13449.
29. Livak KJ, Schmittgen TD. Analysis of relative gene expression data using real-time quantitative PCR and the 2(-Delta Delta C (T)) Method. *Methods*. 2001;25:402-408.
30. Spandidos A, Wang X, Wang H, Seed B. PrimerBank: a resource of human and mouse PCR primer pairs for gene expression detection and quantification. *Nucleic Acids Res*. 2010;38:D792-D799.
31. Song MS, Salmena L, Pandolfi PP. The functions and regulation of the *PTEN* tumour suppressor. *Nature Rev Mol Cell Biol*. 2012;13:283-296.
32. Chen C, Zimmermann M, Tinhofer I, Kaufmann AM, Albers AE. Epithelial-to-mesenchymal transition and cancer stem(-like) cells in head and neck squamous cell carcinoma. *Cancer Lett*. 2013;338:47-56.
33. Yin S, Cheryan VT, Xu L, Rishi AK, Reddy KB. Myc mediates cancer stem-like cells and EMT changes in triple negative breast cancers cells. *PLoS One*. 2017;12:e0183578.
34. Ichikawa T, Nakahata S, Fujii M, Iha H, Morishita K. Loss of NDRG2 enhanced activation of the NF-κB pathway by *PTEN* and *NIK* phosphorylation for ATL and other cancer development. *Sci Rep*. 2015;5:12841.
35. Hu W, Fan C, Jiang P, et al. Emerging role of N-myc downstream-regulated gene 2 (*NDRG2*) in cancer. *Oncotarget*. 2016;7:209-223.
36. Tamura T, Ichikawa T, Nakahata S, et al. Loss of NDRG2 expression confers oral squamous cell carcinoma with enhanced metastatic potential. *Cancer Res*. 2017;77:2363-2374.
37. Taberlay PC, Jones PA. DNA methylation and cancer. *Prog Drug Res*. 2011;67:1-23.
38. Ha PK, Califano JA. Promoter methylation and inactivation of tumour-suppressor genes in oral squamous-cell carcinoma. *Lancet Oncol*. 2006;7:77-82.
39. Almeida LO, Guimaraes DM, Squarize CH, Castilho RM. Profiling the behavior of distinct populations of head and neck cancer stem cells. *Cancers (Basel)*. 2016;8. pii: E7.
40. Nowak DG, Cho H, Herzka T, et al. MYC drives *PTEN/Trp53*-deficient proliferation and metastasis due to IL6 secretion and AKT suppression via PHLPP2. *Cancer Discov*. 2015;5:636-651.

41. Yanagisawa S, Baker JR, Vuppusetty C, et al. Decreased phosphatase *PTEN* amplifies PI3 K signaling and enhances proinflammatory cytokine release in COPD. *Am J Physiol Lung Cell Mol Physiol*. 2017;313:L230-L239.
42. Squarize CH, Castilho RM, Gutkind JS. Chemoprevention and treatment of experimental Cowden's disease by mTOR inhibition with rapamycin. *Cancer Res*. 2008;68:7066-7072.
43. Korkaya H, Paulson A, Charafe-Jauffret E, et al. Regulation of mammary stem/progenitor cells by PTEN/Akt/beta-catenin signaling. *PLoS Biol*. 2009;7:e1000121.
44. Wagner VP, Martins MD, Martins MAT, et al. Targeting histone deacetylase and NF-κB signaling as a novel therapy for mucoepidermoid carcinomas. *Sci Rep*. 2018;8:2065.
45. Wagner VP, Martins MA, Martins MD, et al. Overcoming adaptive resistance in mucoepidermoid carcinoma through inhibition of the IKK-beta/IκBα/NF-κB axis. *Oncotarget*. 2016;7:73032-73044.
46. Squarize CH, Castilho RM, Sriuranpong V, Pinto DS Jr., Gutkind JS. Molecular cross-talk between the NF-κB and STAT3 signaling pathways in head and neck squamous cell carcinoma. *Neoplasia*. 2006;8:733-746.
47. Vasudevan KM, Gurumurthy S, Rangnekar VM. Suppression of *PTEN* expression by NF-κB prevents apoptosis. *Mol Cell Biol*. 2004;24:1007-1021.
48. Xia D, Srinivas H, Ahn YH, et al. Mitogen-activated protein kinase-4 promotes cell survival by decreasing *PTEN* expression through an NF-κB-dependent pathway. *J Biol Chem*. 2007;282:3507-3519.
49. Mayo MW, Madrid LV, Westerheide SD, et al. *PTEN* blocks tumor necrosis factor-induced NF-κB-dependent transcription by inhibiting the transactivation potential of the p65 subunit. *J Biol Chem*. 2002;277:11116-11125.
50. Yang Z, Fang S, Di Y, Ying W, Tan Y, Gu W. Modulation of NF-κB/miR-21/PTEN pathway sensitizes non-small cell lung cancer to cisplatin. *PLoS One*. 2015;10:e0121547.
51. Zhang S, Zhang H, Ghia EM, et al. Inhibition of chemotherapy resistant breast cancer stem cells by a ROR1 specific antibody. *Proc Natl Acad Sci U S A*. 2019;116:1370-1377.
52. Fesler A, Guo S, Liu H, Wu N, Ju J. Overcoming chemoresistance in cancer stem cells with the help of microRNAs in colorectal cancer. *Epigenomics*. 2017;9:793-796.
53. Prieto-Vila M, Takahashi RU, Usuba W, Kohama I, Ochiya T. Drug resistance driven by cancer stem cells and their niche. *Int J Mol Sci*. 2017;18. pii: E2574.
54. Teng Y, Yu X, Yuan H, Guo L, Jiang W, Lu SH. DNMT1 ablation suppresses tumorigenesis by inhibiting the self-renewal of esophageal cancer stem cells. *Oncotarget*. 2018;9:18896-18907.
55. Lee E, Wang J, Yumoto K, et al. DNMT1 regulates epithelial-mesenchymal transition and cancer stem cells, which promotes prostate cancer metastasis. *Neoplasia*. 2016;18:553-566.
56. Momparler RL, Cote S. Targeting of cancer stem cells by inhibitors of DNA and histone methylation. *Expert Opin Investig Drugs*. 2015;24:1031-1043.
57. Gao X, Sheng Y, Yang J, et al. Osteopontin alters DNA methylation through up-regulating DNMT1 and sensitizes CD133 +/CD44+ cancer stem cells to 5 azacytidine in hepatocellular carcinoma. *J Exp Clin Cancer Res*. 2018;37:179.
58. Kwon HM, Kang EJ, Kang K, Kim SD, Yang K, Yi JM. Combinatorial effects of an epigenetic inhibitor and ionizing radiation contribute to targeted elimination of pancreatic cancer stem cell. *Oncotarget*. 2017;8:89005-89020.

Reprint requests:

Rogerio M. Castilho, Laboratory of Epithelial Biology, Department of Periodontics and Oral Medicine, University of Michigan, 1011 North University Avenue, Room 2029 c, Ann Arbor, MI 48109-1078, USA.
rcastilh@umich.edu